Global J. Environ. Sci. Manage. 6(2): 191-202, Spring 2020

Global Journal of Environmental Science and Management
(GJESM)

Homepage: https://www.gjesm.net/

ORIGINAL RESEARCH PAPER

Photocatalytic degradation of ciprofloxacin antibiotic from aqueous solution by $BiFeO_3$ nanocomposites using response surface methodology

R. Mostafaloo[1], M. Asadi-Ghalhari[2]*, H. Izanloo[2], A. Zayadi[3]

[1]*Student Research Committee, Qom University of Medical Sciences, Qom, Iran*

[2]*Research Center for Environmental Pollutants, Qom University of Medical Sciences, Qom, Iran*

[3]*Cellular and Molecular Research Center, Qom University of Medical Sciences, Qom, Iran*

ARTICLE INFO

Article History:
Received 13 June 2019
Revised 22 November 2019
Accepted 1 January 2020

Keywords:
Aqueous Solution
$BiFeO_3$ (BFO)
Ciprofloxacin (CIP)
Magnetic nanocomposites
Photocatalytic degradation
Response surface methodology

ABSTRACT

Ciprofloxacin antibiotic that is used to cure several kinds of bacterial infections have a high solubility capacity in water. The influent of ciprofloxacin to water resources in a low concentration affect the photosynthesis of plants, transforms the morphological structure of the algae, and then disrupts the aquatic ecosystem. 75% of this compound is excreted from the body down to the wastewater which should be removed. $BiFeO_3$, a bismuth-based semiconductor photocatalyst that is responsive to visible light, has been recently used to remove organic pollutants from water. In this study, the optimal conditions for removing ciprofloxacin from aqueous solutions by the $BiFeO_3$ process were investigated. Effective parameters namely pH, reaction time, ciprofloxacin initial concentration, $BiFeO_3$ dose, and temperature on ciprofloxacin removal were studied by using response surface methodology. The validity and adequacy of the proposed model was confirmed by the corresponding statistics (i.e. F-values of 14.79 and 1.67 and p-values of <0.0001 and 0.2505 for the own model and its lack of fit, respectively, R^2 = 0.9107, R^2adjusted = 0.8492, R^2 predicted = 0.70, AP = 16.761). Hence the Ciprofloxacin removal efficiency reached 100% in the best condition (pH 6, initial concentration of 1 mg/L, $BiFeO_3$ dosage of 2.5 g/L, reaction temperature of 30° C, and process time of 46 min).

DOI: 10.22034/gjesm.2020.02.05

NUMBER OF REFERENCES	NUMBER OF FIGURES	NUMBER OF TABLES
46	5	3

*Corresponding Author:
Email: *mehdi.asady@gmail.com*
Phone: : +989122875342
Fax: +98253 7842227

Note: Discussion period for this manuscript open until July 1, 2020 on GJESM website at the "Show Article.

INTRODUCTION

Over the past few years, pharmaceutical residuals have been reported as one of the major environmental concerns throughout the world (Meng *et al.,* 2015). Given the fact that such compounds can change the natural environmental balance, they have been officially labeled as dangerous chemical materials (Ghauch *et al.,* 2009). Among these compounds, antibiotics are used more than any other types of pharmaceutical compounds because of their capability to control human and bestial infections (Jung *et al.,* 2012; Balarak *et al.,* 2016; Zhou *et al.,* 2019). A considerable proportion of antibiotics are excreted from the body after consumption and can pollute aqueous environments (González-Pleiter *et al.,* 2013; Bahramiasl *et al.,* 2015; Amraei *et al.,* 2017). Ciprofloxacin (CIP) is one of the frequently used types of fluoroquinolone group that is used to cure several kinds of bacterial infections. This compound has a high solubility capacity in the water, and 75% of it is excreted from the body down to the sewage system (Githinji *et al.,* 2011). The presence of fluorine atom in this antibiotic makes it more stable in an aqueous environment (Samarghandi *et al.,* 2017). The influent of CIP to aqueous environments in a low concentration affect the photosynthesis of plants, transforms the morphological structure of the algae, and then disrupts the aquatic ecosystem (Samadi *et al.,* 2015). Upon drinking the CIP-polluted water by human beings, the following adverse effects may be observed: anger, nausea, vomiting, headache, diarrhea, and tremor. The high concentration of CIP can cause severe kidney failure and increase liver and thrombocytopenic enzymes (Yoosefian *et al.,* 2016). The concentration of this antibiotic in some of the pharmaceutical wastewater Industries has been measured as 30 mg/L (Samadi *et al.,* 2015). Various methods have been employed to remove pharmaceutical residuals from aqueous environments, such as ozonation, land treatment, Fenton process, ion exchange, nanotubes, and electrocoagulation (Wang *et al.,* 2008; Garoma *et al.,* 2010; Hijosa-Valsero *et al.,* 2011; Samadi *et al.,* 2014; Mostafaloo *et al.,* 2019). The biological treatment is an affordable method, but it is not very effective for persistent organic compounds. Chemical and physical treatments, however, are highly efficient and can produce high-quality effluent; yet, they are also very costly. Thus, researchers are searching for a more appropriate treatment method for pharmaceutical wastewater treatment (Farhadi *et al.,* 2012; Samadi *et al.,* 2015). The photocatalytic process has been regarded as an efficient removal process recently (Xue *et al.,* 2015; Zhou *et al.,* 2018). Photocatalysis involves the photolysis—the breaking down of a chemical by the assistance of light—that is accelerated using a catalyst (Mojir Shaibani *et al.,* 2013). This method, which is considered as a green technology, is an ideal technique to solve environmental impacts and save energy (Di *et al.,* 2014; Zhou *et al.,* 2019). TiO_2 is one of the most popular photocatalysts that is very effective in the photocatalytic destruction of all types of organic pollutants. This photocatalyst can easily degrade organic pollutants into harmless minerals. It should be noted that this photocatalyst only becomes activated under the direct radiation of UV light while about 45% of sunlight turns into visible light and merely 5% into UV light (Di *et al., 2014;* Yin *et al.,* 2016). Therefore, to benefit from solar energy more, it is better to use photocatalysts that are activated by visible light, not UV light (Gao *et al.,* 2007). One of the newest catalysts is $BiFeO_3$ (BFO) that consumes less energy, has a wider contact area, has more chemical stability, and is more recyclable (Mojir Shaibani *et al.,* 2013; Ramezanalizadeh, 2017). BFO crystals can be easily produced by different methods, such as sol-gel method, hydrothermal, and thermal degradation (Ullah *et al.,* 2012). This photocatalyst is a bismuth-based semiconductor that is responsive to visible light and can respond to a smaller bandgap of light than TiO_2 (EV 2/1). Moreover, it has an appropriate piezo-electromagnetic feature that makes it easily degradable at the end of the process (Yuan *et al.,* 2009; Bhaumik *et al.,* 2011; Shariati *et al.,* 2011; Tang 2013; Ramezanalizadeh, 2017). This photocatalyst has been recently used to remove dyes, pesticides, pharmaceutical, and other types of pollutants (Xue *et al.,* 2015; Yin *et al.,* 2016). Overall, previous research shows that in spite of ample advantages, the BFO process has been mostly gone unnoticed in removing and destroying pharmaceutical compounds. Hence, the aim of this study was modeling and optimizing the conditions for removing ciprofloxacin antibiotic from aqueous solutions by the BFO process using response surface methodology (RSM). This study was carried out on a laboratory scale at Qom University of Medical Sciences, Iran, in 2018.

MATERIALS AND METHODS

Chemical materials

Ciprofloxacin ($C_{17}H_{18}FN_3O_3HCl$) was bought from the Canadian company 'Bio Basic Inc'. $Fe(NO_3)_3.9H_2O$، $Bi(NO_3)_3.5H_2O$, ethylene glycol, ethanol, HCl, NaOH, and methanol were obtained from the 'Merk' company. The required concentrations of CIP were prepared based on 1 mg/L stock solution. The pH was adjusted by normal NaOH and HCl solutions and measured by WTW pH meter device, model 7110. The CIP concentration was measured by UV-absorption spectrophotometer (T80 UV/VIS Spectrophotometer, PG Instruments Ltd) within the wavelength of 270.5 nm. The maximum removal efficiency of CIP in the BFO photocatalyst process was calculated based on Eq. 1.

$$\% \text{ removal of CIP} = (C_0 - C_t)/C_0 \times 100 \quad (1)$$

Where, C_0 = CIP concentration in feed solution, C_t = CIP concentration in treated solutions.

BFO synthesis

At first, 0.0016 mol of $Bi(NO_3)_3.5H_2O$ was dissolved in ethylene glycol. Then, to clear and homogenize the attained solution, it was placed in an ultrasonic bath with a temperature of 25° C for two minutes. Afterward, a little Stoichiometry obtained from $Fe(NO_3)_3.9H_2O$ was added to the solution and placed for 10 minutes in an ultrasonic bath with the temperature of 25° C, so that a brownish-red solution was obtained. Next, to make a gel, the solution was placed in an oven with the temperature of 60°C. Finally, to calcinate the obtained solution, the attained gel was placed in 500° C with the rate of 6° C/ min for half an hour (Shaykhi, 2014).

Determining BFO characteristics

The active bands in synthesized BFO were determined by Fourier-transform infrared spectroscopy method (FRIR, Tensor 27 model, Bruker). To dilute the sample, BFO powder was mixed by potassium bromide and then was scanned in 450-4000/cm wavelengths. The superficial morphology of BFO was also determined by electronic microscope scan (SEM, HITACHI-4160 model).

Design and model of experiments based on central composite

Recently many experimental design methods are used to optimize the parameters of different processes. Numerous experiments are required in conventional methods to determine the optimal response, and such methods do not exhibit the combined effect. RSM is a statistical method to design experiments that are used to optimize and analyze the interactional effects of independent factors and reducing the number of experiments in chemical and biochemical process on the other (Shaykhi, 2014; Aravind *et al.,* 2016; Montgomery, 2017). In this study, Design Expert 7 software was employed to the central composite design (CCD) which is an experimental design, useful in response surface methodology. It can analyze different variables (X), such as pH(X_1), X_2 time, the initial concentration of CIP (X_3), temperature (X_4), and BFO dosage (X_5). The design of the central composite makes use of the least-squares technique to perform a model. The number of points in CCD includes central points (C0), axial points (2K), and factorial points (2^k). Therefore, the number of points in the design square was 50, comprising 8 central points, 10 axial points, and 32 factorial points. Table 1 shows the design matrix in the experiments.

Table 1: Coded and actual values of numeric factors

Coded variables (X_i)	Factors (U_i)	Experimental field				
		-□	-1 level	0	+1 level	+□
X_1	A: Solution pH	3	4.5	6	7.5	9
X_2	B: Initial CIP concentration (mg/L)	2	24	46	68	90
X_3	C: BFO Dos (g/L)	1	4.5	8	11.5	15
X_4	D: Reaction time (min)	10	20	30	40	50
X_5	E: Temperature(°C)	0	1.25	2.5	3.75	5

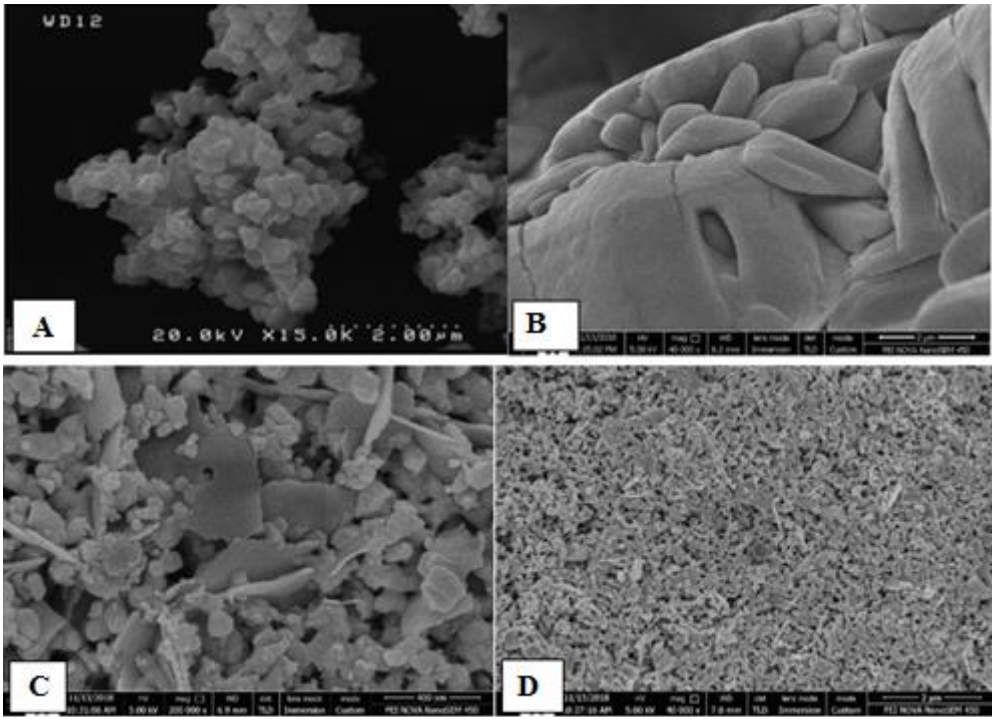

Fig. 1: SEM images (A: BFO image, B: CIP powder, C: BFO image after the reaction, D: BFO image after reaction by 400 nm magnification)

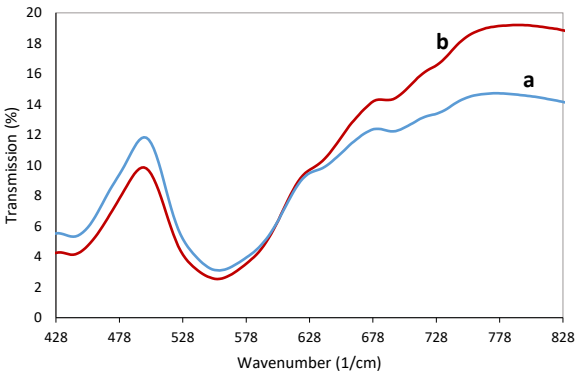

Fig. 2: FTIR spectrum of BFO particles a) before and b) after the reaction

Batch mode experiments

The experiments were conducted in 6 mm/10 ml plates under direct visible light. Batch mode experiments were carried out by adjusting pH (3 to 9 with 0.1 N solutions of HCl or NaOH), initial CIP concentration (1-15 mg/L), and different dosages of BFO (0-5 g/L) within 2 to 90 minutes. In this study, the range of parameters was selected based on the Xue study. (Xue *et al.,* 2015) In order to have a better mixture of the solution and adjusting the reaction temperature (10-50° C), the shaking incubator (JAL TAJHIZ model) was used.

RESULTS AND DISCUSSION

BFO characteristics

The SEM observations from BFO and CIP surfaces before and after reactions are shown in Fig. 1. As shown, CIP particles (A) are almost spherical with a flat surface; the morphology of BFO particles (B) are also flat and spherical without any porosities. The external appearance of BFO particles after the reaction with CIP is shown in the C section of the figure. Based on this image, the CIP surface is covered completely by tiny BFO particles.

The FTIR results obtained from BFO also show two strong adsorption peaks by 441 and 557/cm (Fig. 2). The presence of these peaks is related to the O-Fe-O vibratory bands and tensile Fe-O in the octagonal structure of FeO_6 (Yin *et al.,* 2016; Ramezanalizadeh, 2017). The presence of metal-oxygen compounds proves the formation of Perovskite structure (Wang *et al.,* 2008; Lotey 2014). Changes in the above peaks in the spectra after adsorption of CIP by BFO, indicate the adsorption of ciprofloxacin onto the adsorbent.

Analysis of CCD

The results of central composite design involving five-level central composite designs based on RSM for different surfaces are shown in Table 2. In order to describe the prevailing behavior of the process and the adequacy of the proposed model, the CCD results

Table 2: The 5-factor CCD matrix with coded factor levels for CIP removal based on RSM method

Run order	pH	CIP Concentration (mg/L)	BFO dose (g/L)	Time (min)	Temperature (°C)	Removal Efficiency (%)		
						Obtained	Predicted	Residual
1	4.5	4.5	3.75	24	40	79.35	77.42	1.93
2	6	8	5	46	30	66.28	65.17	1.11
3	4.5	11.5	3.75	68	40	33.2	31.22	1.98
4	6	8	2.5	46	30	37.9	41.31	-3.41
5	6	8	2.5	90	30	19.3	24.86	-5.56
6	4.5	11.5	1.25	24	40	14.19	12.72	1.47
7	7.5	11.5	3.75	24	40	49.56	41.86	7.70
8	6	8	2.5	46	10	25.19	35.79	-10.60
9	6	15	2.5	46	30	27.46	38.38	-10.92
10	4.5	4.5	1.25	68	20	34.35	35.94	-1.59
11	6	8	2.5	46	30	37.14	41.31	-4.17
12	6	8	0	46	30	0	0.48	-0.48
13	7.5	4.5	1.25	24	40	28.06	30.77	-2.71
14	6	8	2.5	2	30	42.97	36.79	6.18
15	7.5	11.5	3.75	68	20	35.37	34.35	1.02
16	6	8	2.5	46	50	35.9	24.67	11.23
17	7.5	11.5	1.25	68	20	19.78	17.84	1.94
18	6	8	2.5	46	30	48.8	41.31	7.49
19	7.5	4.5	1.25	24	20	28.4	33.65	-5.25
20	4.5	4.5	3.75	68	40	74.66	71.73	2.93
21	7.5	4.5	3.75	24	20	59.1	65.80	-6.70
22	6	1	2.5	46	30	100	88.46	11.54
23	6	8	2.5	46	30	54.8	41.31	13.49
24	7.5	11.5	1.25	24	20	25.5	24.07	1.43
25	6	8	2.5	46	30	38.15	41.31	-3.16
26	4.5	11.5	3.75	24	20	51.3	46.56	4.74
27	7.5	4.5	3.75	24	40	64.7	72.41	-7.71
28	6	8	2.5	46	30	37.9	41.31	-3.41
29	4.5	11.5	1.25	68	40	7.2	-1.32	8.52
30	7.5	4.5	3.75	68	40	69.7	69.74	-0.04
31	4.5	4.5	1.25	24	20	45.35	39.02	6.33
32	7.5	4.5	1.25	68	40	23.6	25.95	-2.35
33	9	8	2.5	46	30	38.36	39.40	-1.04
34	4.5	4.5	3.75	24	20	80.44	77.72	2.72
35	6	8	2.5	46	30	38.25	41.31	-3.06
36	7.5	11.5	3.75	24	20	43.37	38.42	4.95
37	6	8	2.5	46	30	36.9	41.31	-4.41
38	4.5	11.5	3.75	68	20	48.02	39.46	8.56
39	4.5	4.5	3.75	68	20	66.08	76.80	-10.72
40	4.5	11.5	1.25	24	20	21.88	25.67	-3.79
41	4.5	11.5	3.75	24	40	28.17	43.09	-14.92
42	4.5	4.5	1.25	24	40	22.91	29.24	-6.33
43	3	8	2.5	46	30	44.65	42.98	1.67
44	7.5	11.5	1.25	24	40	21.18	18.03	3.15
45	7.5	4.5	3.75	68	20	72.85	67.91	4.94
46	4.5	4.5	1.25	68	40	12.9	21.39	-8.49
47	4.5	11.5	1.25	68	20	19.09	16.40	2.68
48	7.5	11.5	1.25	68	40	3.01	7.02	-4.01
49	7.5	4.5	1.25	68	20	42.92	33.59	9.33
50	7.5	11.5	3.75	68	40	28.8	33.01	-4.21

were analyzed. The results of ANOVA and comparison of different models showed that the second model (quadratic) could have a more appropriate behavior in the process (Table 3). Eq. 2 shows the suggested model in an encoded fashion.

The ANOVA results from RSM method showed that the correlation coefficients (R^2), adjusted correlation coefficients (R^2 adjusted), and predicted correlation coefficients (R^2 predicted) were 0.91, 0.85, and 0.70, respectively; given the fact that the difference among these values is less than 0.3, it can be concluded that the obtained and predicted data from the model enjoy an appropriate, exact correlation. Likewise, the AP value was 16.76 showing that the CIP removal model had acceptable reliability. The AP value shows the signal to noise ratio that is an index that proves the efficiency of the model to move in the designed space; values higher than 4 are appropriate for this index (Table 3).

In this study, CIP removal efficiency was optimized with BFO. This optimization with RSM method was used to evaluate the effect of some important variables such as pH, reaction time, initial concentration of CIP, temperature and BFO dosage and their interaction in achieving the optimum conditions in CIP removal efficiency from aqueous solution. Eq. 2. shows the relationship between two dependent variables (CIP removal efficiency) and 5 independent variables. This model was fitted to the response variable from the CCD. Eq. 2 can be employed to evaluate the importance of operational parameters, their interactions, and predictive efficiency of CIP removal in various operational conditions.

Equation 2: CIP removal (%)= $+37.72 - 4.21\ X_1 - 7.73\ X_2 + 26.5\ X_3 + 0.45\ X_4 + 0.65\ X_5 + 0.18\ X_1 X_2 - 0.87\ X_1 X_3 + 0.023\ X_1 X_4 + 0.12\ X_1 X_5 - 1.02\ X_2 X_3 - 0.02\ X_2 X_4 - 0.023\ X_2 X_5 + 0.02\ X_3 X_4 + 0.12\ X_3 X_5 - 0.005\ X_4 X_5 - 0.013\ X_1^2 + 0.45\ X_2^2 - 1.35\ X_3^2 - 0.005\ X_4^2 - 0.028\ X_5^2$ (2)

Effects of process parameters on CIP removal efficiency

Effects of BFO dosage and CIP initial concentration on CIP removal efficiency

Based on Eq. 2, the relationship between CIP removal efficiency and operational parameters is presented as a combination of 5 linear effects, 10 mutual effects, and 5 second-rate effects. The most effective parameter in CIP removal was the BFO dosage that had the highest positive coefficient in the equation. Fig. 3 shows the perturbation graph for CIP removal parameters. In accordance with this graph, it is possible to compare the effects of various parameters on the removal response by keeping variables constant on particular points in the design space under RSM method. In this graph, the steep slope or curve of each parameter shows how sensitive the response is to each parameter.

As observed in the graph, the BFO dosage parameter (code C) is in a form of a positive steep slope and the initial concentration of ciprofloxacin (code B) is in a form of a negative steep slope, showing the higher sensitivity of the removal process to these two variables. The perturbation graph clearly shows the individual effects of each parameter; yet, it cannot show the interactional effects among variables. The 3D response surface plot under RSM method for the interactions between dos of BFO and concentration of CIP are presented in Fig 4. In this graph, the mutual effect of the initial concentration of CIP and BFO dosage is shown. It is observed that a decrease in the initial concentration of CIP and an increase in BFO dosage could enhance the removal efficiency. As shown in the graph, a decrease in the initial concentration from 11.5 to 4.5 mg/L and an increase in BFO dosage from 1.25 to 3.37 g/L could increase the CIP removal efficiency from 20.07 to

Table 3. ANOVA for the second-order model of CIP removal by BFO from CCD based on RSM method

Source	Sum of squares	Degree freedom	Mean Square	F-value	p-value
Model	20209.57	20	1010.48	14.79	< 0.0001
Residual	1981.15	29	68.32		
Lack of Fit	1663.68	22	75.62	1.67	0.2505
Pure Error	317.47	7	45.35		
Cor Total	22190.72	49			

R^2 = 0.9107, R^2adjusted = 0.8492, R^2predicted = 0.70, AP =16.761

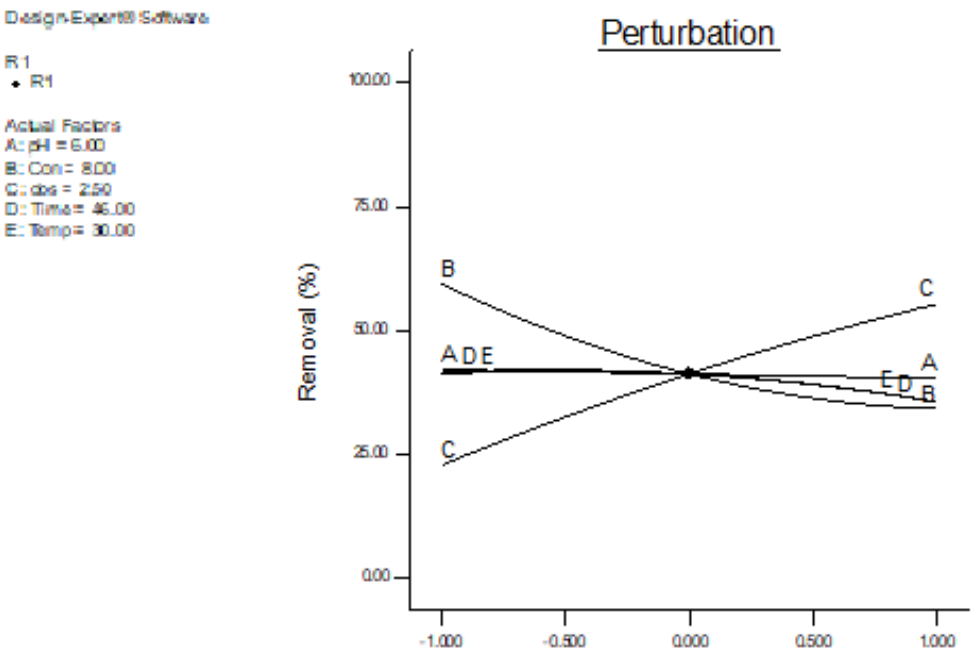

Fig. 3: The perturbation graph for experiments' parameters on CIP removal efficiency under RSM method

34.52 and 48.97%, respectively. Similarly, the lowest concentration level of CIP and highest BFO dosage increased the removal efficiency of the process up to 77.86%.

The observed decrease in the removal efficiency of CIP initial concentrations can be attributed to the saturation, a decrease in active surface places and light penetration, and an increase in light dispersion in BFO surface (Elmolla, 2010). Moreover, an increase in BFO dosage can increase active surface places and provided a wider contact area between CIP and photocatalyst. Parsa et al. also observed similar results regarding the effects of these parameters on the removal of pollutants in their studies (Parsa *et al.,* 2016).

Reaction time effects on CIP removal efficiency

As depicted in the perturbation graph (Fig. 3), increasing the reaction time by 46 min enhanced the removal efficiency; the removal efficiency trend, however, was decreasing beyond that time. The fast removal in the initial reaction stages can be attributed to the existence of more active places on the BFO surface. Nevertheless, such places are saturated after a while. Likewise, as the time and saturation of active places increase, the light penetration in BFO surface decreases and reduces the photocatalytic performance (Roy *et al.,* 2014; Roy *et al.,* 2017). These findings are all in agreement with the observations of Samadi *et al.* (2015; Yoosefian *et al.* (2016); Amraei *et al.* (2017) and Samarghandi *et al.* (2017).

PH effects on CIP removal efficiency

pH is one of the most important variables in this study due to its effect on surface properties of the substance. Therefore, with the increase in pH, the efficiency of CIP removal is also reduced. The best performance is achieved at pH equal to 6. As shown in Fig. 5a the CIP ionizing molecule has two proton binding sites, including the carboxylic acid group (pK_a1 = 6.1) and the amine group (pK_a2 = 8.7). Thus, in accordance with Fig. 5b, the dominant form of CIP at pH < 6.1 is in the cationic form, due to the protonation of the amine group, and at pH>8.7 in the form of anion, due to loss of the proton from the carboxylate group, and at 6.1<pH<8.7 is neutral. Given the measurement of zeta potential, the BFO isoelectric point (the pHpzc was 6.7 for BFO) in a lower pH than the surface charge of pH-pzc was positive. Therefore, in pH 6, the BFO surface charge

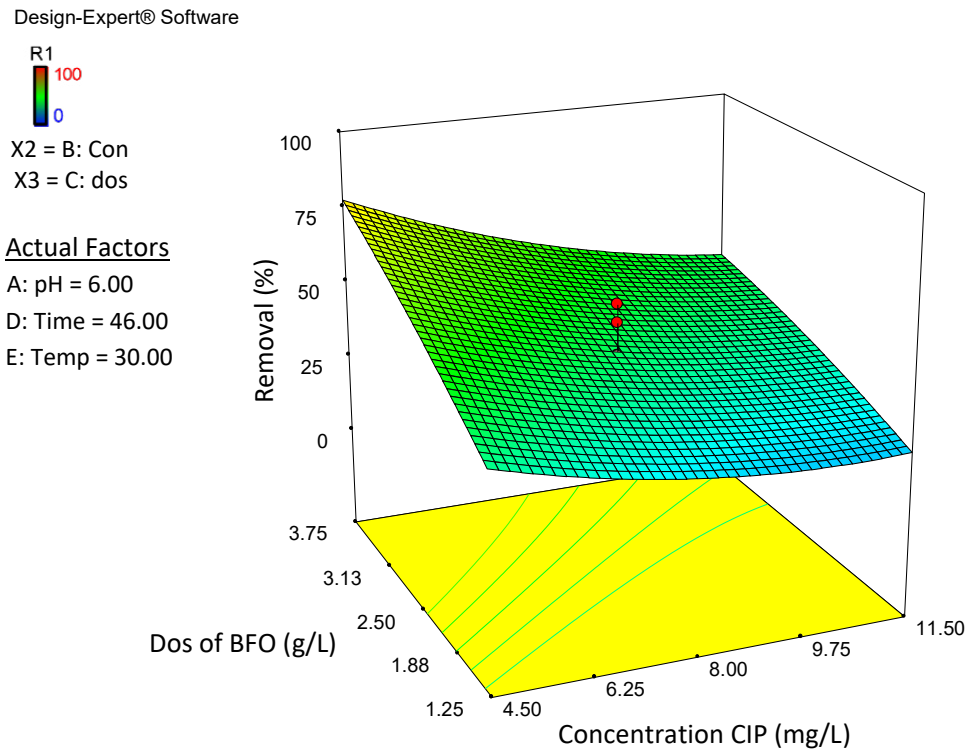

Fig.4: The 3D response surface plot of the mutual effects of CIP initial concentration and BFO dosage on removal efficiency under RSM method

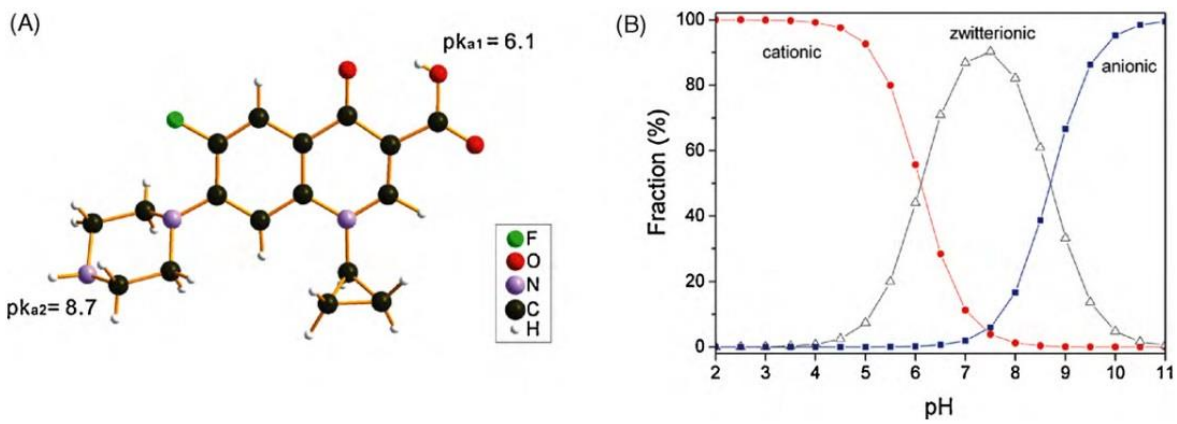

Fig. 5: A) Molecular structure of ciprofloxacin, B) ionizing forms of ciprofloxacin at different pH (Wang *et al.*, 2010)

was positive and CIP charge was mostly in the form of a positive charge with little neutral and negative charge as shown in Fig. 5b. Thus, because of the positive-positive electrostatic among CIP and BFO in the optimal pH, the possibility of CIP removal in the adsorption process based on electrostatic interactions of ions is weaker. On the other hand, given the below equations for the photocatalytic process, the photocatalytic process is more efficient in pH levels beyond 4.88 based on Eq. 3. (Xue *et al.*, 2015). Hence, it seems that the dominant process for CIP removal by BFO is photocatalytic.

$$PC \xrightarrow{h\nu} h^+ + e^- \ (PC: photocatalyst)$$

$$H_2O + h^+ \rightarrow \cdot OH + H^+$$

$$OH^- + h^+ \rightarrow \cdot OH$$

$$O_2 + e^- \rightarrow \cdot O_2^-$$

$$O_2^- + H^+ \rightarrow \cdot HO_2 \ (pk_a = 4.88) \quad (3)$$

$$HO_2 + \cdot HO_2 \rightarrow H_2O_2 + O_2$$

$$O_2^- + \cdot HO_2 \rightarrow HO_2^- + O_2$$

$$HO_2^- + H^+ \rightarrow H_2O_2$$

In line with the findings of this study, Zhaohui *et al.* (2011) observed that the best pH level for the removal of CIP by kaolinite ranged from 5 to 8. In their study, the pHpzc kaolinite amount was determined as 4. In another study, Samadi *et al.* (2015) investigated CIP removal efficiency by Fe_3O_4/MWCNT. They found that since the surface charge of Fe_3O_4/MWCNT and CIP in pH 4 were respectively negative and positive, the optimal pH was 4.

Effects of temperature on CIP removal efficiency

Contrary to what Homem *et al.* (2010) and Fakhri *et al.* (2014) reported, based on the output perturbation graph from RSM method (Fig. 3) in this study, it was observed that increasing the temperature up to 30 ˚C could enhance the efficiency of the process. It is probable that the efficiency increase in the removal process follows Arrhenius law in which a rise in temperature can increase particle movement and the possibility of BFO particles contacting CIP ions.

CONCLUSION

RSM method helped to optimize the process parameters with a minimum number of experiments, as well as analyzed the interaction between the parameters. In this study we optimized the efficiency of removing ciprofloxacin antibiotic from aqueous environments using BFO photocatalyst as a green technology with RSM method. The experiments were conducted based on CCD statistical procedures. According to the overall findings and ANOVA results, the best prediction model is the second-rate model. The relationship between CIP removal efficiency and operational parameters is presented as a combination of 5 linear effects, 10 mutual effects, and 5 second-rate effects based on optimized model under RSM method. The most effective parameter in CIP removal was the BFO dosage that had the highest positive coefficient in the equation. The best composite response for the ciprofloxacin removal was observed in pH 6, initial concentration of 1 mg/L, BFO dosage of 2.5 g/L, reaction temperature of 30˚ C, and process time of 46 min; the removal efficiency reached 100% in the above-mentioned conditions. In conclusion, the high efficiency of antibiotic removal by BFO proves that this process can be successfully employed to remove ciprofloxacin antibiotic from aqueous environments. Although BFO was successfully applied to remove CIP from aqueous solutions, its degradation should be studied in much lower concentrations as it detected in the natural aqueous solutions. Other factors' effect such as acute toxicity assays, mineralization degree, interfering species, working with real wastewater effluent, etc. should also be paid for more investigations.

AUTHOR CONTRIBUTIONS

Throughout the study performance; M. Asadi-Ghalhari performed the literature review, experimental design, analyzed and interpreted the data, prepared the manuscript text, and manuscript edition. R. Mostafaloo performed the experiments and literature review, compiled the data and manuscript preparation. H. Izanloo helped in the literature review and manuscript preparation. A. Zayadi performed some of the remained experiments.

ACKNOWLEDGMENT

Authors would like to thank Qom University of Medical Sciences, in supporting the current study.

CONFLICT OF INTEREST

The author declares that there is no conflict of interests regarding the publication of this manuscript. In addition, the ethical issues, including plagiarism, informed consent, misconduct, data fabrication and/or falsification, double publication and/or submission, and redundancy have been completely observed by the authors.

ABBREVIATIONS

(%)	percentage
°C	Degree Celsius
3D	Three dimensional
ANOVA	Analysis of variance
AP	Access Points
BFO	$BiFeO_3$
$Bi(NO_3)_3.5H_2O$	Bismuth(III) Nitrate Pentahydrate
CCD	Central composite design
Con.	Concentration
Dos	Dosage
eV	Electron volt
H_2O_2	Hydrogen Peroxide
$Fe(NO_3)_3.9H_2O$	Iron(III) Nitrate Nonahydrate
Fe_3O_4/MWCNT	Multi-walled carbon nanotube (MWCNT) and magnetite
FTIR	Fourier-transform infrared spectroscopy
g/L	Gram per liter
HCl	Hydrogen chloride
mg/L	Milligram per liter
Mol	The mole
NaOH	Sodium hydroxide
O_2	Molecular Oxygen
pH	Potential of Hydrogen
pK_a	Acid dissociation constant
PZC	Point of zero charge
R^2	Coefficient of determination
RSM	Response surface methodology
SEM	scanning electron microscope
Temp	Temperature
UV/VIS	Ultraviolet visible

REFERENCES

Amraei, B.; Rezaei Kalantary, R.; Jonidi Jafari, A.; Gholami, M., (2017). Efficiency of CuFe2O4 bimetallic in removing amoxicillin from aqueous solutions. J. Mazandaran Univ. Med. Sci., 27(147): 259-275 **(17 pages).**

Aravind, J., Kanmani, P., Sudha, G., Balan, R., (2015). Optimization of chromium (VI) biosorption using gooseberry seeds by response surface methodology. Global J. Environ. Sci. Manage., 2(1): 61-68 **(8 pages).**

Azargohar, R.; Dalai, A., (2005). Production of activated carbon from Luscar char: experimental and modeling studies. Micropor. Mesopor. Mat., 85(3):219-25. **(7 pages).**

Bahrami Asl, F.; Kermani, M.; Farzadkia, M.; Esrafili, A.; Salahshour Arian, S.; Zeynalzadeh, D., (2015). Removal of metronidazole from aqueous solution using ozonation process. J. Mazandaran Univ. Med. Sci., 24(121): 131-140 **(10 pages).**

Balarak, D.; Mostafapour, F.; Joghataei, A., (2016). Experimental and kinetic studies on Penicillin G adsorption by Lemna minor. Br. J. Pharm. Res., 9(5): 1-10 **(10 pages).**

Ehera, SK.; Meena, H.; Chakraborty, S.; Meikap, B., (2018). Application of response surface methodology (RSM) for optimization of leaching parameters for ash reduction from low-grade coal. Int. J. Mining Sci. Technol., 28(4): 621-9 **(9 pages).**

Bhaumik, M.A.; Maity,A.; Srinivasu, V.; Onyango, M., (2011). Enhanced removal of Cr (VI) from aqueous solution using polypyrrole/Fe3O4 magnetic nanocomposite. J. hazard. Mater., 190(1): 381-390 **(10 pages).**

Di, L.; Yang, G.; Xian, J.; Ma, J.; Jiang, R.; Wei, Z., (2014). Enhanced photocatalytic activity of BiFeO3 particles by surface decoration with Ag nanoparticles. J. Mater. Sci. - Mater. Electron., 25(6): 2463-2469 **(7 pages).**

Elmolla, E.S.; Chaudhuri, M., (2010). Photocatalytic degradation of amoxicillin, ampicillin and cloxacillin antibiotics in aqueous solution using UV/TiO2 and UV/H2O2/TiO2 photocatalysis. J. Desalination. 252(1–3): 46-52 **(7 pages).**

Fakhri, A.; Adami, S., (2014). Adsorption and thermodynamic study of Cephalosporins antibiotics from aqueous solution onto MgO nanoparticles. J. Taiwan Inst. Chem. Eng., 45(3): 1001-1006 **(6 pages).**

Farhadi, S.; Aminzadeh, B.; Torabian, A.; Khatibikamal, V.; Fard, M., (2012). Comparison of COD removal from pharmaceutical wastewater by electrocoagulation, photoelectrocoagulation, peroxi-electrocoagulation and peroxi-photoelectrocoagulation processes. J. hazard. Mater., 219: 35-42 **(8 pages).**

Gao, F.; Chen, X.; Yin, K.; Dong, S.; Ren, Z.; Yuan, F.; Yu, T.; Zou, Z.; Liu, J., (2007). Visible-Light Photocatalytic Properties of Weak Magnetic BiFeO3 Nanoparticles. Adv. Mater., 19(19): 2889-2892 **(4 pages).**

Garoma, T.; Umamaheshwar, S.K.; Mumper, A., (2010). Removal of sulfadiazine, sulfamethizole, sulfamethoxazole, and sulfathiazole from aqueous solution by ozonation. Chemosphere., 79(8): 814-820 **(7 pages).**

Ghauch, A.; Tuqan, A.; Assi, H., (2009). Antibiotic removal from water: Elimination of amoxicillin and ampicillin by microscale and nanoscale iron particles. Environ. Pollut., 157(5): 1626-1635 **(10 pages).**

Githinji, L. J.; Musey, M.K.; Ankumah, R.O., (2011). Evaluation of the fate of ciprofloxacin and amoxicillin in domestic wastewater. Water Air Soil Pollut., 219(1-4): 191-201 **(10 pages).**

González-Pleiter, M.; Gonzalo, S.; Rodea-Palomares, I.; Leganés, F.; Rosal, R.; Boltes, K.; Marco, E.; Fernández-Piñas, F., (2013). Toxicity of five antibiotics and their mixtures towards photosynthetic aquatic organisms: Implications for environmental risk assessment. Water Res., 47(6): 2050-2064 **(15 pages).**

Hijosa-Valsero, M.; Fink, G.; Schlüsener, M.; Sidrach-Cardona, R.; Martín-Villacorta, J.; Ternes, T.; Bécares, E., (2011). Removal of antibiotics from urban wastewater by constructed wetland optimization. Chemosphere. 83(5): 713-719 **(7 pages).**

Homem, V.; Alves, A.; Santos, L., (2010). Amoxicillin degradation at ppb levels by Fenton's oxidation using design of experiments. Sci. Total Environ., 408(24): 6272-6280 **(9 pages).**

Jung, Y.; Gi Kim, G.; Yoon, Y.; Kang, J.; Hong, Y.; Wook Kim, H., (2012). Removal of amoxicillin by UV and UVH2O2 processes. Sci. Total Environ: 160-167 **(8 pages).**

Lotey, G.S.; Verma, N., (2014). Synthesis and characterization of BiFeO3 nanowires and their applications in dye-sensitized solar cells. Mater. Sci. Semicond. Process., 21: 206-211 **(6 pages).**

Meng, L.-W.; Li, X.; Wang, K.; Ma, K.L.; Zhang, J., (2015). Influence of the amoxicillin concentration on organics removal and microbial community structure in an anaerobic EGSB reactor treating with antibiotic wastewater. Chem. Eng. J., 274: 94-101 **(8 pages).**

Mojir Shaibani, P.; Prashanthi, K.; Sohrabi, A.; Thundat, T., (2013). Photocatalytic BiFeO3 nanofibrous mats for effective water treatment. J. Nanotechnol: 1-7 **(7 pages).**

Montgomery, D.O.,(2017). Design and analysis of experiments, john wiley and sons **(630 pages).**

Mostafaloo, R.; Mahmoudian, M.H.; Asadi-Ghalhari, M., (2019). BiFeO3/Magnetic Nanocomposites for the Photocatalytic Degradation of Cefixime from Aqueous Solutions under visible light. J. Photochem. Photobiol., 382:111926- 111933 **(8 pages).**

Mostafaloo, R.; Yari, A.R.; Mohammadi, M.J.; Khaniabadi, Y.O.; Asadi-Ghalhari, M., (2019). Optimization of the electrocoagulation process on the effectiveness of removal of Cefixime antibiotic from aqueous solutions. Desalination. Water Treat., 144: 138-144 **(7 pages).**

Parsa, J. B.; Panah, T.M.; Chianeh, F.N., (2016). Removal of ciprofloxacin from aqueous solution by a continuous flow electro-coagulation process. Korean J. Chem. Eng., 33(3): 893-901 **(11 pages).**

Ramezanalizadeh, H., (2017). Design, preparation and characterization of a novel BiFeO3/CuWO4 heterojunction catalyst for one-pot synthesis of trisubstituted imidazoles. Iran Chem. Commun., 1-17 **(17 pages).**

Roy, P.; Dey, U.; Chattoraj, S.; Mukhopadhyay, D.; Mondal, N., (2017). Modeling of the adsorptive removal of arsenic (III) using plant biomass: a bioremedial approach. Appl. Water Sci., 7(3): 1307-1321 **(15 pages).**

Roy, P.; Mondal, N.; Das, K., (2014). Modeling of the adsorptive removal of arsenic: a statistical approach. J. Environ. Chem. Eng., 2(1): 585-597 **(18 pages).**

Samadi, M.T.; Shokoohi, R.; Araghchian, M.; Tarlani Azar, M., (2014). Amoxicillin Removal from Aquatic Solutions Using Multi-Walled Carbon Nanotubes. J. Mazandaran Univ. Med. Sci., 24(117): 103-115 **(13 pages).**

Samadi, M.T.; Shokoohi, R.; Harati, R., (2015). Evaluation of Synthesized Fe3O4/MWCNTs Nanocomposite Used in the Heterogeneous Fenton Process for the Removal of Ciprofloxacin Antibiotic. J. Water Wastewater., (5): 80-89 **(10 pages).**

Samarghandi, M.; Ahmadisoost, G.H.; Shabanloo, A.; Majidi, S.; Rezaee Vahidian, H.; Maroufi, S.; Shahmoradi, M.; Mehralipour, J., (2017). Optimization of Electrocoagulation via Response Surface Methodology to Remove Ciprofloxacin from Aqueous Media. J. Water Weastewater., 28(2): 12-21 **(10 pages).**

Shariati, S.; Faraji, M.; Yamini, Y.; Rajabi, A.A., (2011). Fe3O4 magnetic nanoparticles modified with sodium dodecyl sulfate for removal of safranin O dye from aqueous solutions. J. Desalination. 270(1): 160-165 **(6 pages).**

Shaykhi, Z.M.; Zinatizadeh, A., (2014). Statistical modeling of photocatalytic degradation of synthetic amoxicillin wastewater (SAW) in an immobilized TiO2 photocatalytic reactor using response surface methodology (RSM). J. Taiwan Inst. Chem. Eng., 45(4): 1717-1726 **(10 pages).**

Tang, S.C.; Lo, L.M., (2013). Magnetic nanoparticles: essential factors for sustainable environmental applications. Water Res., 47(8): 2613-2632 **(20 pages).**

Ullah, I.; Ali, s.; Hanif, M.A.; Shahid, S.A., (2012). Nanoscience for environmental remediation: a review. Int .J .Chem. Biochem. sci., 2(1): 60-77 **(18 pages).**

Wang, Y.-J.; Jia, D.A.; Sun, R.J.; Zhu, H.W.; Zhou, D.M., (2008). Adsorption and cosorption of tetracycline and copper (II) on montmorillonite as affected by solution pH. Environ. Sci. Technol., 42(9): 3254-3259 **(6 pages).**

Wang, C-J.; Li, Z.; Jiang, W-T.; Jean, J-S.; Liu, C-C., (2010). Cation exchange interaction between antibiotic ciprofloxacin and montmorillonite. J. Hazard. Mater., 183(1-3): 309-314 **(6 pages).**

Xue, Z.; Wang, T.; Chen, B.; Malkoske, T.; Yu, S.; Tang, Y., (2015). Degradation of Tetracycline with BiFeO3 Prepared by a Simple Hydrothermal Method. Mater., 8(9): 6360-6378 **(19 pages).**

Yin, J.; Liao, G.; Zhou, J.; Huang, C.; Ling, Y.; Lu, P.; Li, L., (2016). High performance of magnetic BiFeO3 nanoparticle-mediated photocatalytic ozonation for wastewater decontamination. Sep. Purif. Technol., 168: 134-140 **(7 pages).**

Yoosefian, M.; Ahmadzadeh, S.; Aghasi, M.; Dolatabadi, M., (2016). Optimization of electrocoagulation process for efficient removal of ciprofloxacin antibiotic using iron electrode; kinetic and isotherm studies of adsorption. J. Mol. Liq., 225: 544-553 **(10 pages).**

Yuan, P.; Fan, M.; Yang, D.; He, H.; Liu, D.; Yuan, A.; Zhu, J.; Chen, T., (2009). Montmorillonite-supported magnetite nanoparticles for the removal of hexavalent chromium [Cr (VI)] from aqueous solutions. J. Hazard. Mater., 166(2): 821-829 **(9 pages).**

Zhaohui, L.; Hanlie, H.; Libing, L.; Caren, J.; Ackleyc, L.; Schulzc, R,; Emard, M., (2011). A mechanistic study of ciprofloxacin removal by kaolinite. Colloids Surf., B., 88 88: 339-344 **(6 pages).**

Zhou, C.; Huang, D,; Xu, P.; Zeng, G.; Huang, J.; Shi, T,; Lai, C.; Zhang, C.; Cheng, M.; Lu, Y., (2019). Efficient visible light driven degradation of sulfamethazine and tetracycline by salicylic acid modified polymeric carbon nitride via charge transfer. Chem. Eng. J., 370: 1077-1086 **(10 pages).**

Zhou, C.; Lai, C.; Huang, D.; Zeng, G.; Zhang, C.; Cheng, M.; Hu, L.; Wan, J.; Xiong, W.; Wen, M.; (2018). Highly porous carbon nitride by supramolecular preassembly of monomers for photocatalytic removal of sulfamethazine under visible light driven. Appl. Catal., B., 220: 202-210 **(9 pages).**

Zhou, C.; Xu, P.; Lai, C.; Zhang, C.; Zeng, G.; Huang, D.; Cheng, M.; Hu, L.; Xiong, W.; Wen, X., (2019). Rational design of graphic carbon nitride copolymers by molecular doping for visible-light-driven degradation of aqueous sulfamethazine and hydrogen evolution. Chem. Eng. J., 359: 186-196 **(11 pages).**

AUTHOR (S) BIOSKETCHES

Mostafaloo, R., MSc. Student Research Committee, Qom university of Medical Sciences, Qom, Iran. Email: *r.moostafaloo@gmail.com*

Asadi-Ghalhari, M., Ph.D., Assistant Professor, Research Center for Environmental Pollutants, Qom University of Medical Sciences, Qom, Iran. Email: *mehdi.asady@gmail.com*

Izanloo, H., Ph.D., Assistant Professor, Research Center for Environmental Pollutants, Qom University of Medical Sciences, Qom, Iran. Email: *hizan52@gmail.com*

Zayadi, A., M.Sc., Cellular and Molecular Research Center, Qom University of Medical Sciences, Qom, Iran. Email: *zayadiasma@yahoo.com*

HOW TO CITE THIS ARTICLE

Mostafaloo, R.; Asadi-Ghalhari, M.; Izanloo, H.; Zayadi, A., (2020). Modeling and optimization of the photocatalytic degradation of ciprofloxacin antibiotic from aqueous solution by $BiFeO_3$ nanocomposites. Global J. Environ. Sci. Manage., 6(2): 191-202.

DOI: 10.22034/gjesm.2020.02.05

url: https://www.gjesm.net/article_37695.html